frontiers | Frontiers in Earth Science

TYPE Original Research
PUBLISHED 18 September 2025
DOI 10.3389/feart.2025.1691323

OPEN ACCESS

EDITED BY
Pengfei Liu,
CCCC Second Harbor Engineering Co., Ltd., China

REVIEWED BY
Yang Cao,
Fuzhou University, China
Pei Huang,
Chang'an University, China
Wei HE,
North China University of Water Resources and Electric Power, China

*CORRESPONDENCE
Jingxi Zhang,
zjx_adhere@gs.zzu.edu.cn

RECEIVED 23 August 2025
ACCEPTED 03 September 2025
PUBLISHED 18 September 2025

CITATION
Wang R, Li S, Li C, Bian K and Zhang J (2025) Mechanistic analysis of TBM cutterhead-ground interaction under mud build-up effect.
Front. Earth Sci. 13:1691323.
doi: 10.3389/feart.2025.1691323

Mechanistic analysis of TBM cutterhead-ground interaction under mud build-up effect

Renchong Wang[1], Shiwei Li[2,3], Congshi Li[1], Ke Bian[2,3] and Jingxi Zhang[4]*

[1]Henan Qianping Reservoir Irrigation District Project Company, Luoyang, Henan, China, [2]Henan Provincial Water Conservancy Technology Application Center, Zhengzhou, Henan, China, [3]Henan Key Laboratory of Safety Technology for Water Conservancy Project, Zhengzhou, Henan, China, [4]School of Water Conservancy and Transportation, Zhengzhou University, Zhengzhou, Henan, China

Introduction: In tunnel construction using TBMs, the complex mineral composition of strata and hydrogeological conditions often induce cutterhead mud build-up, which results in sharp increases in torque and thrust, thereby reducing excavation efficiency. Understanding the interaction between the TBM cutterhead and the surrounding ground under cutterhead blockage conditions is therefore a critical challenge for improving tunnelling efficiency.
Methods: This study develops a cutterhead load model that explicitly incorporates both aperture ratio and mud coating effects, and establishes a load-prediction framework for TBM excavation in composite strata.
Results: The validity of the proposed model is verified using field monitoring data. On this basis, the influence of aperture ratio on excavation loads is systematically analysed.
Discussion: An optimization strategy—maintaining a relatively large aperture ratio—is proposed to enhance TBM tunnelling efficiency, providing effective theoretical support and practical guidance for addressing cutterhead mud build-up.

KEYWORDS

composite strata, cutterhead mud build-up, cutterhead load, aperture ratio, TBM excavation efficiency

1 Introduction

With the advantages of safety and efficiency, tunnel boring machines (TBMs) have been widely used in tunnelling tunnels of various sizes (Hassanpour et al., 2011). Its performance largely depends on the rock breaking efficiency induced by its cutterhead, which bears complex loads due to the difficult grounds, such as fault zone, blocky rock mass and mixed face (Zhao et al., 2007). Many tunnelling projects driven by different types of TBMs suffered from inadequate cutterhead loads (Bilgin and Algan, 2012; Jancsecz et al., 1999; Nelson et al., 1992). Therefore, calculation and prediction of cutterhead loads are crucially important for a successful TBM tunnelling.

Precise control of shield tunneling loads relies on understanding the cutterhead-soil interaction. This interaction comprises two main components: the cutting action between the cutter and the soil, and the extrusion between the cutterhead faceplate and the soil

(Han et al., 2017; Li et al., 2022). The resistance encountered by the tool while cutting the soil primarily contributes to the cutterhead torque, while the interaction between the cutterhead faceplate and the soil mainly generates thrust resistance for the shield (Hasanpour et al., 2018; Wang et al., 2022).

Researchers have conducted extensive work on cutterhead-soil interaction to establish a reasonable theoretical calculation model for tunneling loads (Guo et al., 2018; Ramoni and Anagnostou, 2010) employed numerical simulation to study the thrust force requirements for tunnel boring machines (TBMs) in squeezing ground (Shi et al., 2011). further determined the composition of cutterhead torque and proposed a calculation method considering cutterhead structure, cutting principle, and the interaction between the cutterhead and soil (Wang et al., 2012). improved the Krause model for estimating cutterhead thrust by incorporating five main components, validating it through laboratory tests with a U1.8 m EPB shield tunneling machine.

To analyze the excavation load of layered soil (Sun et al., 2018; Zhang et al., 2015; Zhang et al., 2014; Zhang et al., 2016), proposed a load model that considers the properties and thickness of each soil layer. Ates et al. (2014) established a statistical model between cutterhead diameter and total installed load on the basis of a database containing 262 types of TBMs and emphasized the key role of geological parameters in the prediction of total loads. Zhou and Zhai, (2018) presented a theoretical model for the cutterhead torque of an EPB TBM in soft ground. Geng et al. (2016), Liu et al. (2018) developed a load prediction model on the basis of the CSM model and the disc cutter layout. Jing et al. (2019), Zhao et al. (2019) reported a power function relationship between rock breaking load and joint parameters on the basis of *in-situ* data and full-scale rotary cutting tests, and established a load prediction model. Liu et al. (2020) conducted a series of novel rolling cutting tests on layered sandstone, and the influence of dip angle, strata, normal force, and rotational speed on the reliability of the disc cutter were analyzed. Wang et al. (2022) propose a novel thrust model that incorporates soil properties, shield operating parameters, pose parameters, and geometric parameters to estimate total and grouped thrusts, and its effectiveness is validated through a case study. Shen et al. (2025) significantly contributes to the understanding and quantification of shield tunneling thrust and cutterhead torque by establishing a refined three-dimensional cutter-soil interaction model. Zhang et al. (2025) incorporated the mud build-up effect into the load model in their study.

Although numerous studies have focused on load prediction models in shield tunnelling, few have explicitly considered the effects of mud build-up, which decreases the cutterhead aperture ratio and consequently alters excavation loads. To address this limitation, this study develops a load prediction model that incorporates the effective aperture ratio of the cutterhead, quantitatively evaluates its impact on excavation loads, and proposes corresponding optimization strategies. The proposed model is applicable to various ground conditions, and the findings provide theoretical support and practical guidance for improving excavation efficiency and ensuring construction safety under mud build-up scenarios.

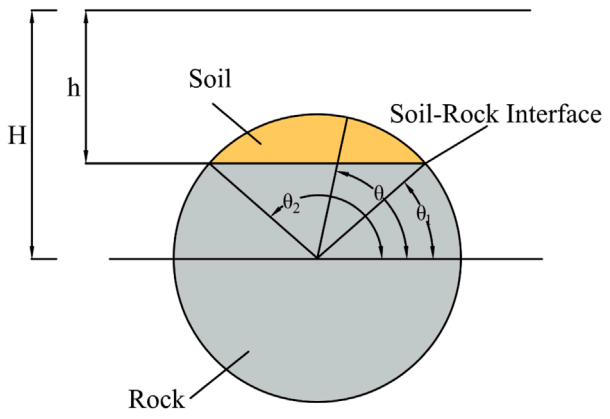

FIGURE 1
Schematic diagram of composite strata at the TBM excavation face.

2 Interaction between the TBM cutterhead and the strata considering mud build-up

2.1 TBM thrust force

The load analysis of cutterhead mud build-up is critical for tunnel design and construction. The mud build-up effect causes raised deposits on the cutterhead surface, altering the contact area and pressure distribution between the cutterhead and the ground, which in turn affects both torque and thrust. By analyzing the load characteristics under mud build-up conditions, the influence on cutterhead torque and thrust can be quantified, providing a basis for the rational determination of design and construction parameters to ensure tunneling safety and efficiency.

2.1.1 Shield TBM cutterhead thrust considering mud clogging

Kong et al. (2022), using a soft-over-hard stratum as an example, conducted a mechanical analysis of TBM tunneling considering factors such as ground composition, cutter geometry, TBM advance rate, and cutterhead torque (Figure 1). Based on this, a thrust calculation method for TBM tunneling in composite strata was proposed, yielding expressions F_1 and F_2.

The lateral earth pressure acting on the cutterhead faceplate is discussed based on the position of the soil–rock interface on the TBM excavation face, as shown in Equations 1–3.

$$F_{1s} = \int_{\theta_1}^{\theta_2} \int_{\frac{H-h}{\sin\theta}}^{\frac{D}{2}} (H - r\sin\theta)\lambda_1\gamma_1 r\mathrm{d}r\mathrm{d}\theta \tag{1}$$

$$F_{1r} = \lambda_2 \left\{ \begin{aligned} &\int_0^{2\pi} \int_0^{\frac{D}{2}} \left[\gamma_1\left(H - \frac{D}{2}\right) + \gamma_2\left(\frac{D}{2} - r\sin\theta\right)\right] r\mathrm{d}r\mathrm{d}\theta - \\ &\int_{\theta_1}^{\theta_2} \int_{\frac{H-h}{\sin\theta}}^{\frac{D}{2}} \left[\gamma_1\left(H - \frac{D}{2}\right) + \gamma_2\left(\frac{D}{2} - r\sin\theta\right)\right] r\mathrm{d}r\mathrm{d}\theta \end{aligned} \right\} \tag{2}$$

Based on the above equation, the lateral pressure acting on the cutterhead faceplate in the soil and rock zones can be calculated. Considering the influence of mud build-up on the actual aperture ratio during cutterhead excavation, the resulting force F_1 can be expressed as:

$$F_1 = (1\text{-}\xi')(F_{1s} + F_{1r}) \tag{3}$$

Where:

F_1 is the lateral earth pressure acting on the cutterhead faceplate in composite strata.

F_{1s} is the lateral earth pressure from the upper soil layer acting on the faceplate.

F_{1r} is the lateral earth pressure from the lower rock layer acting on the faceplate.

ξ' is the actual aperture ratio of the cutterhead during excavation, considering the effect of mud build-up.

θ is the dip angle between the soil-rock interface on the excavation face and the horizontal direction through the shield center.

θ_1, θ_2 are angular parameters related to the soil–rock interface.

r is the distance from a point on the cutterhead to the cutterhead center.

D is the diameter of the cutterhead.

h is the burial depth of the soil-rock interface on the excavation face.

H is the burial depth of the shield's central axis.

λ_1 is the lateral earth pressure coefficient of the soil.

λ_2 is the lateral earth pressure coefficient of the rock.

γ_1 is the unit weight of the soil.

γ_2 is the unit weight of the rock.

2.1.2 Shield–stratum frictional resistance

The frictional force between the upper soil and the shield casing can be expressed as Equation 4:

$$F_{2s} = \mu_1 DL \int_{\theta_1}^{\frac{\pi}{2}} p_{s1} \sin\theta + p_{s2} \cos\theta \mathrm{d}\theta \tag{4}$$

The frictional force between the lower rock mass and the shield casing can be expressed as Equation 5:

$$F_{2r} = \mu_2 DL \left[\int_0^{\theta_1} P_{r1} \sin\theta + P_{r2} \cos\theta \mathrm{d}\theta + \int_{-\frac{\pi}{2}}^{0} P_{r2} \cos\theta\text{-}P_{r1} \sin\theta \mathrm{d}\theta \right] \tag{5}$$

The value of F_2 can be expressed as Equation 6:

$$F_2 = F_{2s} + F_{2r} \tag{6}$$

Where:

F_2 is the frictional resistance between the shield shell and the ground during shield advancement.

F_{2s} is the frictional force between the upper soil layer and the shield shell.

F_{2r} is the frictional force between the lower rock layer and the shield shell.

P_{s1} and P_{s2} are the vertical and horizontal pressures exerted by the upper soil layer on the shield shell.

P_{r1} and P_{r2} are the vertical and horizontal pressures exerted by the lower rock layer on the shield shell.

μ_1 is the friction coefficient between the soil and the shield shell.

μ_2 is the friction coefficient between the rock and the shield shell.

L is the length of the shield shell.

2.1.3 Penetration resistance acting on the cutters mounted on the cutterhead

In composite strata, the TBM cutterhead no longer only considers its interaction with a single soil type. Depending on the stratigraphic conditions during TBM tunneling, both the rolling cutters and disc cutters interact with the soil and rock during the cutting and rock-breaking process. Zhang et al. (2025) considered the cutter forces under mud build-up conditions as shown in Equation 7.

$$F_3 = \sum_{i=1}^{n} f_{ni} \tag{7}$$

Where:

F_3 is the resistance force acting on the cutter during penetration.

f_{ni} is the penetration resistance force acting on a single cutter under mud build-up conditions in contact with the rock stratum.

2.2 Cutterhead torque

2.2.1 Cutterhead face–stratum frictional resistance torque

Zhu et al. (2014) calculated based on the soil and rock masses in the TBM excavation interface region, as shown in Equations 8–10:

$$T_{1s} = (1\text{-}\xi')\mu_1\lambda_1\gamma_1 \int_{\theta_1}^{\theta_2} \int_{\frac{H\text{-}h}{\sin\theta}}^{\frac{D}{2}} (H\text{-}r\sin\theta) r^2 \mathrm{d}r\mathrm{d}\theta \tag{8}$$

$$T_{1r} = (1\text{-}\xi')\mu_2\lambda_2 \left\{ \begin{array}{l} \int_0^{2\pi} \int_0^{\frac{D}{2}} \left[\gamma_1 \left(H\text{-}\frac{D}{2} \right) + \gamma_2 \left(\frac{D}{2}\text{-}r\sin\theta \right) \right] r^2 \mathrm{d}r\mathrm{d}\theta - \\ \int_{\theta_1}^{\theta_2} \int_{\frac{H\text{-}h}{\sin\theta}}^{\frac{D}{2}} \left[\gamma_1 \left(H\text{-}\frac{D}{2} \right) + \gamma_2 \left(\frac{D}{2}\text{-}r\sin\theta \right) \right] r^2 \mathrm{d}r\mathrm{d}\theta \end{array} \right\} \tag{9}$$

The resistive torque T_1 between the cutterhead faceplate and the surrounding geological formation is given by:

$$T_1 = T_{1s} + T_{1r} \tag{10}$$

Where:

T_1 is the torque generated by friction between the cutterhead front face and the surrounding ground.

T_{1s} is the torque generated by friction between the cutterhead front face and the soil.

T_{1r} is the torque generated by friction between the cutterhead front face and the rock.

b is the thickness of the cutterhead.

2.2.2 Cutterhead side–stratum frictional resistance torque

Liu et al. (2015) and Zhu et al. (2014) calculated based on the soil and rock masses in the TBM excavation interface region, as shown in Equations 11–13:

$$T_{2s} = \frac{\mu_1 \gamma_1 b D^2}{4} \int_{\theta_1}^{\theta_2} \left[\left(H - \frac{D}{2} \sin\theta \right) \sin^2\theta + \lambda_1 \left(H - \frac{D}{2} \sin\theta \right) \cos^2\theta \right] \mathrm{d}\theta \tag{11}$$

$$T_{2r} = \frac{\mu_2 \gamma_2 b D^2}{4} \left\{ \begin{array}{l} \int_{0}^{\theta_1} \left[\left(H - \frac{D}{2} \sin\theta \right) \sin^2\theta + \lambda_2 \left(H - \frac{D}{2} \sin\theta \right) \cos^2\theta \right] \mathrm{d}\theta + \\ \int_{\theta_2}^{2\pi} \left[\left(H - \frac{D}{2} \sin\theta \right) \sin^2\theta + \lambda_2 \left(H - \frac{D}{2} \sin\theta \right) \cos^2\theta \right] \mathrm{d}\theta \end{array} \right\} \tag{12}$$

The resistive torque T_2 between the cutterhead side and the surrounding geological formation is given by:

$$T_2 = T_{2s} + T_{2r} \tag{13}$$

Where:

T_2 is the torque generated by friction between the cutterhead side and the surrounding ground.

T_{2s} is the torque generated by friction between the cutterhead side and the soil.

T_{2r} is the torque generated by friction between the cutterhead side and the rock.

T_3 is the torque generated by friction between the back of the cutterhead and the muck.

2.2.3 Cutterhead back–excavated material frictional resistance torque

As shown in Equation 14.

$$T_3 = (1 - \xi') \int_0^{2\pi} \int_0^{\frac{D}{2}} \mu_1 F_{\mathrm{li}} r^2 \mathrm{d}r\mathrm{d}\theta \tag{14}$$

Where:

F_{li} is the muck pressure acting on a micro-element at the back of the cutterhead (Liu et al., 2015).

R_{i} is the contact radius of the disc cutter, i.e., the distance from the disc cutter contact point to the rotation axis.

R_{j} is the contact radius of the scraper, i.e., the distance from the scraper contact point to the rotation axis.

2.2.4 Cutterhead torque induced by ground resistance during cutter excavation

As shown in Equation 15.

$$T_{41} = \sum_{i=1}^{n} f_{\mathrm{ti}} R_{\mathrm{i}} \tag{15}$$

Where:

T_4 is the torque generated by the resistance of the ground against cutter penetration on the cutterhead (Zhang et al., 2025).

f_{ni} is the tangential force acting on a single cutter under mud build-up conditions in contact with the stratum.

3 Engineering case verification

3.1 Project overview

This study takes a TBM tunnel section in Shenzhen as the engineering background. The tunnel was excavated by an earth pressure balance (EPB) shield through strata composed of cobble soil, gravel soil, coarse sand, sandy strongly weathered granite, and moderately weathered granite, forming a typical "soft-over-hard" composite ground. During excavation, frequent mud build-up was observed on the cutterhead, particularly when crossing the interface between gravel soils and sandy strongly weathered granite. Such composite strata share similarities with karst-affected geological conditions in southern China, where unconsolidated sediments overlie hard bedrock, often accompanied by groundwater activity and localized dissolution features. A composite cutterhead was adopted for the TBM, with an overall aperture ratio of 35% and a central aperture ratio of 38%. The cutterhead was equipped with six 18-inch double-edged disc cutters at the center and thirty-two 18-inch single-edged disc cutters. In addition, ninety-four scrapers were installed, along with twelve edge scrapers.

3.2 Engineering data analysis

3.2.1 Load model verification

Using the load calculation formulas presented in Chapter 2, the thrust and torque were calculated, and the relationships between the measured and theoretical values of thrust and torque within the cutterhead mud build-up zone were plotted, as shown in Figures 2, 3.

Within the actual cutterhead mud build-up zone, the average measured total thrust of the TBM machine was 16,372.05 kN, while the theoretical value was 17,499.55 kN, approximately 6.8% higher. This discrepancy arises because the theoretical thrust calculation assumes simultaneous contact between all cutters and the ground, whereas in practice, due to vertical differences between disc cutters and scrapers and variations in installation positions even among the same cutter type, cutter-ground contact does not occur simultaneously. The average measured total torque was 3,585.67 kN m, while the theoretical value was 4,113.32 kN m, about 14.7% higher. This larger deviation is primarily related to the axial coverage of the mud build-up on the cutterhead: when the mud build-up completely covers the cutters and prevents them from cutting the ground, the torque required for cutting must be comprehensively reconsidered.

For the analysis of forces acting on the cutterhead face, variations in aperture ratio under different levels of mud build-up are introduced to more accurately evaluate the cutterhead loading. In the cutter load calculation, this study considers the cutter forces under mud build-up conditions. In summary, the proposed load calculation model is applicable to various typical ground conditions and demonstrates strong generality and engineering adaptability.

3.2.2 Formation process of mud build-up

During the tunneling process from ring 0 to ring 165, the TBM advance rate is shown in Figure 4, in conjunction with the thrust and torque variations illustrated in Figures 2, 3. Based on the variation curves of relevant parameters during excavation, the formation

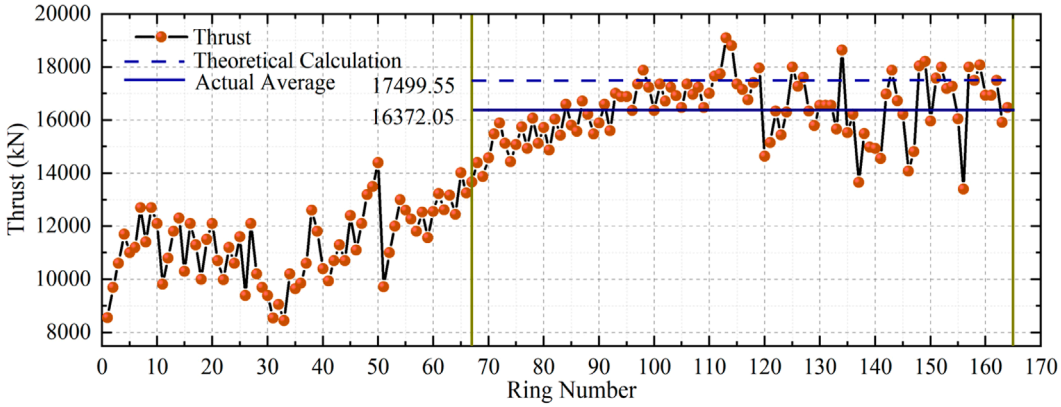

FIGURE 2
Thrust comparison curve.

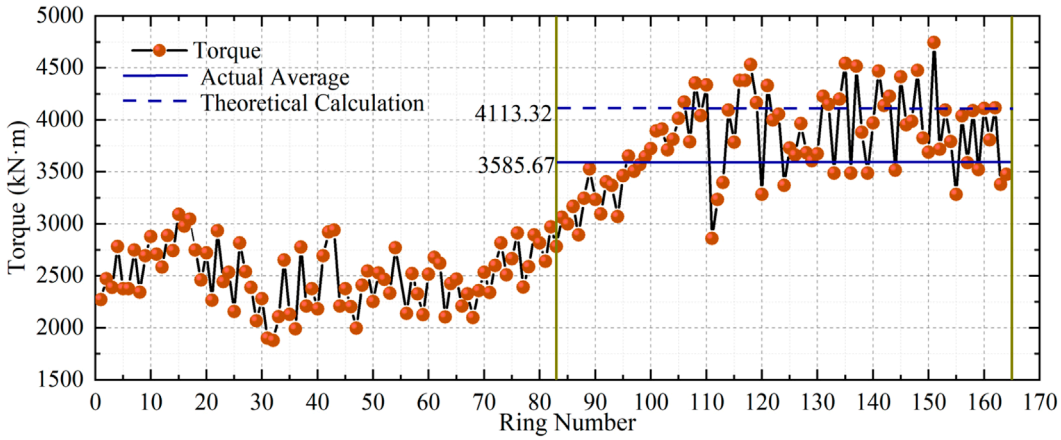

FIGURE 3
Torque comparison curve.

process of cutterhead mud build-up can be divided into five stages, as analyzed below:

3.2.2.1 Normal Excavation Stage

From ring 0 to ring 67, excluding the initial increase in advance rate and thrust caused by TBM start-up, all tunneling parameters remained stable with relatively small fluctuations. During this stage, the TBM advance rate ranged from 20 to 40 mm/min, the thrust ranged from 8,000 to 15,000 kN, and the cutterhead torque ranged from 1,750 to 3,000 kN m.

3.2.2.2 Mud Build-up Formation Stage

Between rings 67 and 68, abnormal changes in tunneling parameters were observed. Except for the cutterhead torque, which remained stable, the advance rate dropped sharply while the thrust increased and showed a tendency to exceed the stable range observed during rings 0 to 67. At this stage, mud build-up began to form on the cutterhead, particularly around the openings, reducing the aperture ratio and impeding the discharge of excavated muck. Meanwhile, mud build-up on the spokes and faceplates of the cutterhead introduced additional resistance, resulting in increased thrust. However, since the degree of cutterhead mud build-up was still relatively low, its impact on cutting performance was limited, allowing the cutterhead torque to remain stable despite the reduced advance rate.

3.2.2.3 Expansion Stage of Mud Build-up on Cutterhead Face

From ring 68 to ring 81, the advance rate no longer declined but fluctuated within a relatively stable range of 10–25 mm/min. The thrust continued to increase but at a slower rate than in the previous stage, ranging from 14,000 to 18,000 kN. The cutterhead torque remained stable during this phase.

3.2.2.4 Full Coverage Stage of Cutterhead Mud Build-up

From ring 81 to ring 90, the cutterhead torque rose sharply from 2,196 kN m to 4,274 kN m. At this point, extensive mud build-up had formed on the cutterhead, accumulating in thickness along the tunneling direction. The build-up gradually extended inward from the periphery, covering previously unobstructed openings. As

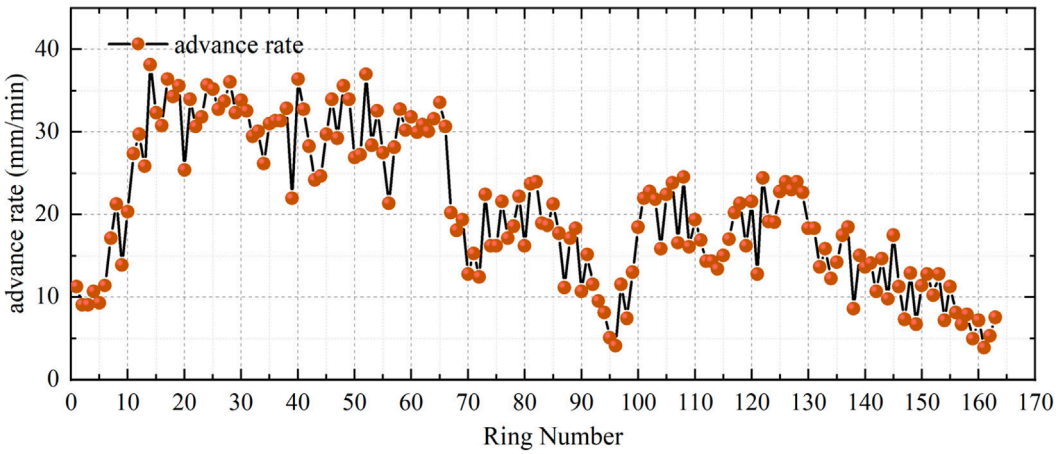

FIGURE 4
Advance rate variation curve.

a result, the cutters experienced reduced cutting capacity due to the mud coverage, and the excavated muck became increasingly difficult to discharge through the blocked openings. These combined effects led to a rapid and significant increase in cutterhead torque.

3.2.2.5 Stabilized Mud Build-up Stage

After ring 90, the thrust stabilized within the range of 14,000 to 19,000 kN, and the cutterhead torque remained between 3,000 and 4,500 kN m. Analysis indicates that by this stage, the cutterhead face and openings were completely covered by mud build-up, effectively forming a secondary "cutterhead" composed of the accumulated mud. Under the combined effects of adhesion and friction with the excavation face, the mud build-up reached a mechanical equilibrium, and its scale ceased to grow. The contact condition between the cutterhead, cutters, and the surrounding soil mass became stable, resulting in a steady state of thrust and torque during excavation.

Based on the variation of tunneling parameters during the cutterhead mud build-up process, rings 56 to 110-covering the transitional phases-were selected for further analysis of thrust and torque.

The thrust variation curve for rings 56 to 110 is shown in Figure 5.

Within this interval, the TBM thrust exhibited a gradual increase with the tunneling progress. Around ring 90, the growth trend of thrust approached zero and remained stable thereafter. This indicates that in the earlier stage, the increasing thrust was caused by the progressive accumulation of mud build-up on the cutterhead surface, which led to greater resistance between the cutterhead face, cutters, and the excavation face. To maintain excavation, the TBM thrust was gradually increased. Once the mud build-up on the cutterhead surface reached its maximum extent, it effectively replaced direct contact between the cutterhead and the ground, resulting in a stabilized interaction and consistent thrust in the subsequent stage.

The variation curve of cutterhead torque for rings 56 to 110 is shown in Figure 6.

The cutterhead torque within this interval showed a gradual increase with the tunneling progress, with the rate of increase becoming more pronounced over time. This suggests that cutterhead mud build-up had a greater impact on torque than on thrust. Due to the presence of mud build-up on the cutterhead surface, the cutting performance of the shield cutters was significantly impaired. Meanwhile, the accumulated mud intensified friction between the cutterhead and the excavation face. To maintain excavation, the cutterhead had to generate higher torque to meet the basic cutting requirements.

3.3 Analysis of cutterhead aperture ratio variation

3.3.1 Relationship between cutterhead aperture ratio and loads

According to the stages of cutterhead mud build-up defined in Section 3.2.2, both the cutterhead aperture ratio and the mud build-up coverage ratio on the cutterhead vary continuously throughout the TBM tunneling process. Based on this, the corresponding variation curves can be plotted as follows:

Since the cutterhead remains in constant contact with the excavation face during actual tunneling, it is not possible to monitor the aperture condition of the cutterhead in real time. Therefore, the following assumptions are made:

1. The mud build-up coverage on the cutterhead openings and faceplates is assumed to increase linearly and uniformly, without considering abrupt changes in adhesion due to specific strata conditions;
2. The mud build-up on the cutterhead surface is considered to be in a dynamic equilibrium between detachment and adhesion. In other words, the mud already adhered to the cutterhead is assumed to remain unchanged as tunneling progresses, ensuring that the amount of mud build-up on the openings and faceplates increases monotonically.

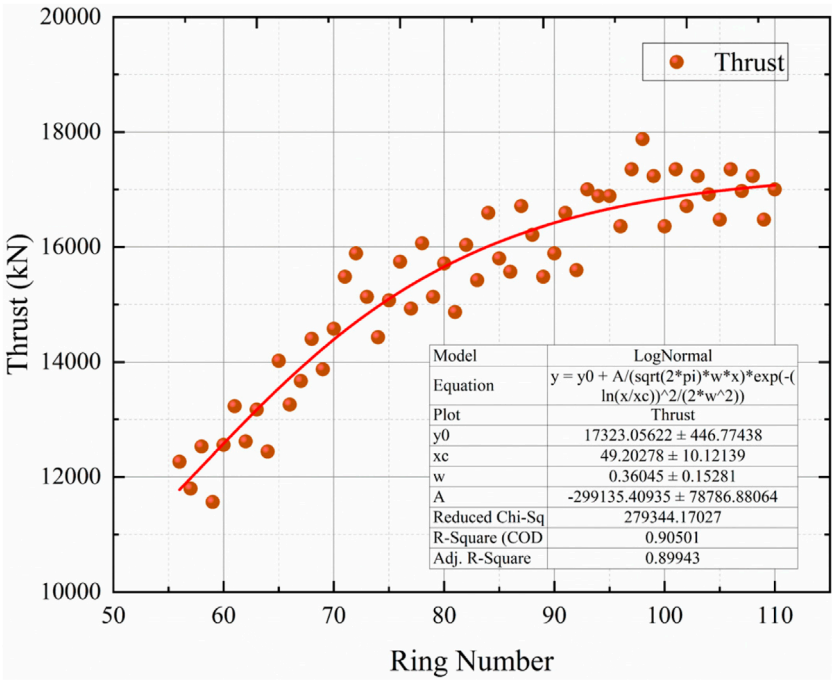

FIGURE 5
Fitted curve of TBM thrust for rings 56 to 110.

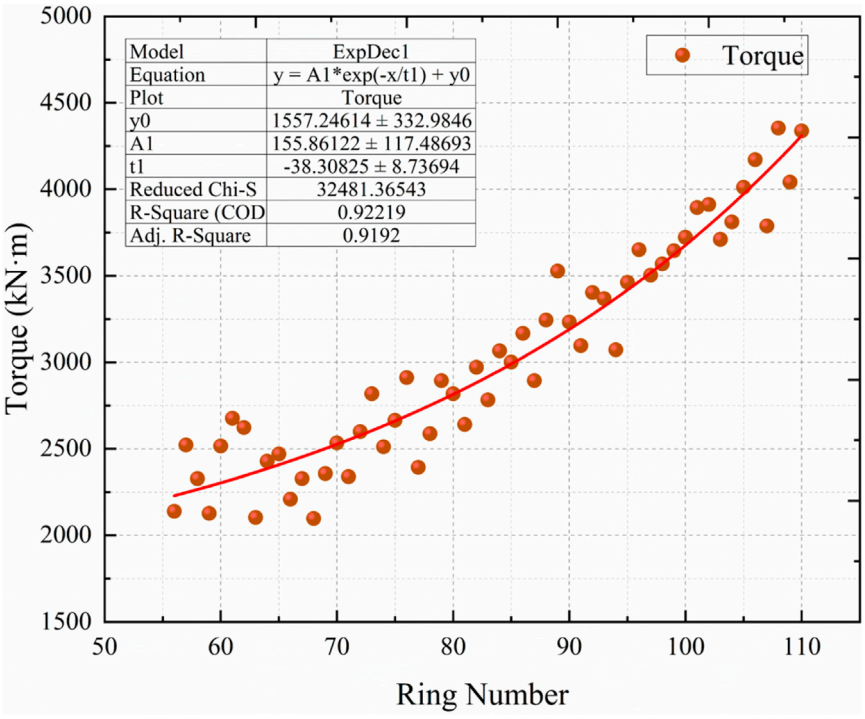

FIGURE 6
Fitted curve of cutterhead torque for rings 56 to 110.

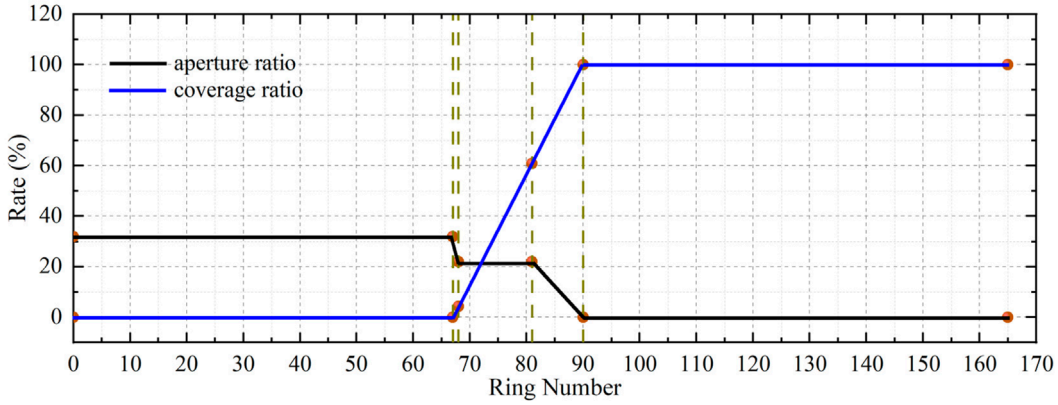

FIGURE 7
Evolution of cutterhead mud build-up.

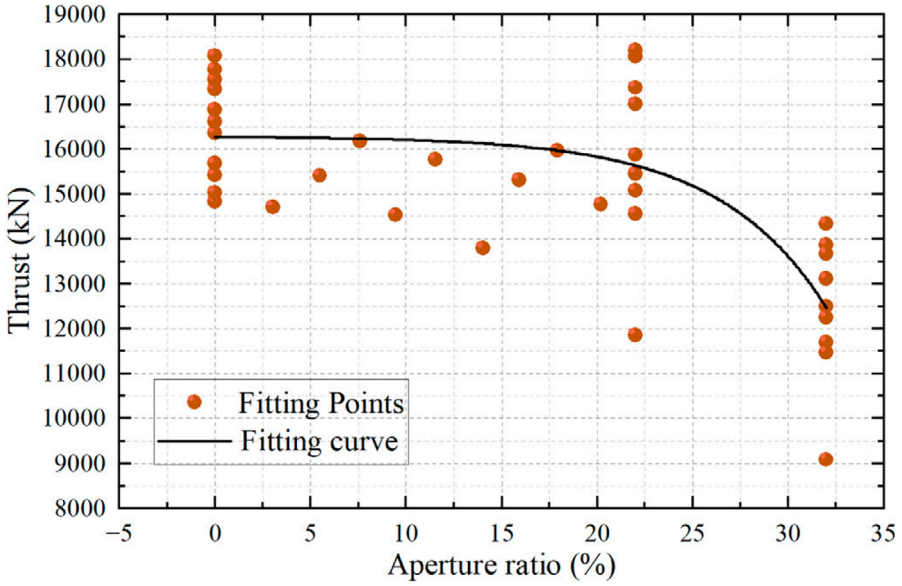

FIGURE 8
Correlation between TBM thrust and aperture ratio in presence of cutterhead mud build-up.

Based on the above assumptions, the variation curves of the aperture ratio in the presence of cutterhead mud build-up and the mud build-up coverage ratio on the cutterhead during rings 0 to 165 are shown in Figure 7.

As shown in Figure 7, significant changes in the cutterhead aperture ratio in the presence of mud build-up and the mud build-up coverage ratio occurred between rings 67 and 90. During this interval, the overall mud build-up coverage on the cutterhead continuously increased, as the mud coating on the faceplate expanded radially outward from the center of the cutterhead. The aperture ratio in the presence of cutterhead mud build-up exhibited two stages of decline and one stage of stabilization. According to the mud build-up obstruction model at the cutterhead openings (Ruyong, 2018; Yongjian, 2020), the mud coating over the openings may undergo bending failure. Once the mud build-up in the openings reaches an upper limit, the aperture ratio becomes stable due to mechanical equilibrium at the openings. However, when thick mud build-up accumulates around the opening areas, it gradually expands axially along the cutterhead, eventually filling all remaining openings.

To further analyze the relationship between the aperture ratio in the presence of cutterhead mud build-up and tunneling parameters during TBM excavation, the correlation between TBM thrust and the aperture ratio is illustrated in Figure 8.

As shown in Figure 8, there is a clear correlation between TBM thrust and the aperture ratio in the presence of cutterhead mud build-up. When the cutterhead face is only partially covered by mud build-up-i.e., when the aperture ratio is relatively high-the TBM thrust remains low. As the aperture ratio decreases and

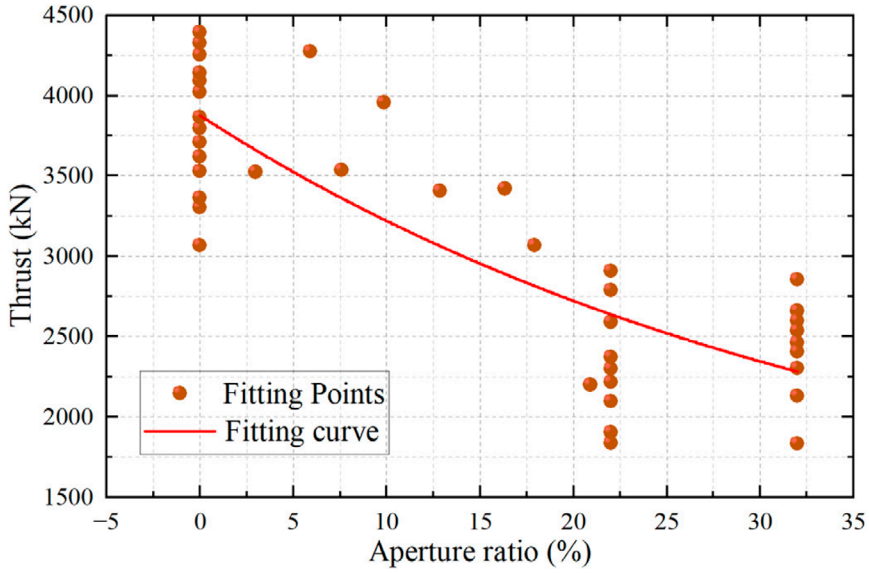

FIGURE 9
Correlation between cutterhead torque and aperture ratio in presence of cutterhead mud build-up.

the cutterhead becomes fully covered by mud build-up, the thrust approaches its maximum value.

To further analyze the relationship between the aperture ratio in the presence of cutterhead mud build-up and tunneling parameters during TBM excavation, the correlation between cutterhead torque and the aperture ratio is illustrated in Figure 9.

As shown in Figure 9, a clear negative correlation is observed between cutterhead torque and the aperture ratio. When the aperture ratio is relatively high, the cutterhead torque remains low. As the aperture ratio decreases to its minimum—indicating complete coverage of the cutterhead by mud build-up—the cutterhead torque reaches its maximum value.

These results suggest that the aperture ratio under cutterhead mud build-up conditions provides valuable insight into the behavior of tunneling parameters. Selecting a cutterhead design with a relatively large aperture ratio during the planning stage can effectively reduce the risk of cutterhead mud build-up.

3.3.2 Optimization recommendations based on aperture ratio

The cutterhead aperture ratio not only affects muck discharge efficiency but is also closely related to the stability of mud build-up formation at the openings. Based on the aperture ratio analysis, it is recommended to maximize the aperture ratio within the structural constraints of the cutterhead to reduce the likelihood of muck accumulation and subsequent mud build-up in the opening areas. From a topological perspective, the location of the openings also influences mud build-up formation. The central region of the cutterhead poses a higher risk of cutterhead mud build-up; therefore, it is advisable to allocate larger openings near the center, while closed structural elements such as spokes, ribs, and faceplates-hich are essential for maintaining excavation face stability-hould be arranged closer to the cutterhead perimeter.

4 Conclusion

The mud build-up effect can cause abrupt changes in TBM loads, thereby reducing tunneling efficiency. In this study, a load prediction framework for TBM tunneling in composite strata under mud build-up conditions was established, and a cutterhead load model incorporating both the aperture ratio and mud coverage was proposed. Field monitoring data were employed to validate the framework, and the influence of aperture ratio on tunneling efficiency was systematically analyzed. The main conclusions are as follows:

A cutterhead load calculation model that accounts for the actual aperture ratio was developed, which effectively captures the influence of mud build-up on cutterhead loads.

Mud build-up was incorporated into the analysis of cutterhead–strata interaction, demonstrating its significant impact on cutter forces and excavation loads.

Increasing the cutterhead aperture ratio is shown to improve tunneling efficiency, providing an effective strategy to mitigate the adverse impacts of mud build-up.

The proposed model and findings not only enhance the understanding of mud build-up mechanisms in TBM tunneling but also offer theoretical support and practical guidance for safe and efficient construction in karst-affected composite strata.

Data availability statement

The original contributions presented in the study are included in the article/supplementary material. Further inquiries can be directed to the corresponding author.

Author contributions

RW: Conceptualization, Validation, Writing – original draft. SL: Resources, Writing – original draft. CL: Software, Writing – original draft. KB: Writing – review and editing, Visualization. JZ: Writing – review and editing.

Funding

The author(s) declare that financial support was received for the research and/or publication of this article. This research was supported by the Henan Qianping Irrigation District North Trunk Canal Ruyang Water Supply Project (Grant No. QPRY-ZX-2024-01), the 2024 Henan Water Conservancy Science and Technology Project (Grant No. GG202455), and the National Natural Science Foundation of China (Grant No. 52079128).

Conflict of interest

Authors RW and CL were employed by Henan Qianping Reservoir Irrigation District Project Company. Authors SL and KB were employed by Henan Provincial Water Conservancy Technology Application Center. Authors SL and KB were also employed by Henan Key Laboratory of Safety Technology for Water Conservancy Project. Author JZ was employed by the School of Water Conservancy and Transportation, Zhengzhou University.

Generative AI statement

The author(s) declare that no Generative AI was used in the creation of this manuscript.

Any alternative text (alt text) provided alongside figures in this article has been generated by Frontiers with the support of artificial intelligence and reasonable efforts have been made to ensure accuracy, including review by the authors wherever possible. If you identify any issues, please contact us.

Publisher's note

References

Ates, U., Bilgin, N., and Copur, H. (2014). Estimating torque, thrust and other design parameters of different type TBMs with some criticism to TBMs used in Turkish tunneling projects. *Tunn. Undergr. Space Technol.* 40, 46–63. doi:10.1016/j.tust.2013.09.004

Bilgin, N., and Algan, M. (2012). The performance of a TBM in a squeezing ground at Uluabat, Turkey. *Tunn. Undergr. Space Technol.* 32, 58–65. doi:10.1016/j.tust.2012.05.004

Geng, Q., Wei, Z., Meng, H., and Macias, F. J. (2016). Mechanical performance of TBM cutterhead in mixed rock ground conditions. *Tunn. Undergr. Space Technol.* 57, 76–84. doi:10.1016/j.tust.2016.02.012

Guo, K., Xu, Y., and Li, J. (2018). Thrust force allocation method for shield tunneling machines under complex load conditions. *Automation Constr.* 96, 141–147. doi:10.1016/j.autcon.2018.08.016

Han, M. D., Cai, Z. X., Qu, C. Y., and Jin, L. S. (2017). Dynamic numerical simulation of cutterhead loads in TBM tunnelling. *Tunn. Undergr. Space Technol.* 70, 286–298. doi:10.1016/j.tust.2017.08.028

Hasanpour, R., Rostami, J., Thewes, M., and Schmitt, J. (2018). Parametric study of the impacts of various geological and machine parameters on thrust force requirements for operating a single shield TBM in squeezing ground. *Tunn. Undergr. Space Technol.* 73, 252–260. doi:10.1016/j.tust.2017.12.027

Hassanpour, J., Rostami, J., and Zhao, J. (2011). A new hard rock TBM performance prediction model for project planning. *Tunn. Undergr. Space Technol.* 26 (5), 595–603. doi:10.1016/j.tust.2011.04.004

Jancsecz, S., Krause, R., and Langmaack, L. (1999). "Advantages of soil conditioning in shield tunneling: experiences of LRTS Izmir," in Proceedings of the World Tunnel Congress '99, Oslo, June 1999, 865–875.

Jing, L.-j., Li, J.-b., Yang, C., Chen, S., Zhang, N., and Peng, X.-x. (2019). A case study of TBM performance prediction using field tunnelling tests in limestone strata. *Tunn. Undergr. Space Technol.* 83, 364–372. doi:10.1016/j.tust.2018.10.001

Kong, X., Tang, L., Ling, X., Tang, W., and Zhang, Y. (2022). Thrust calculation method for earth pressure balance shield in Compound strata. *Chin. J. Undergr. Space Eng.* 18 (06), 1805–1813.

Li, J., Zhang, B., Lyu, D., Guo, J., Su, K., and Hu, B. (2022). Fatigue reliability analysis of tunnelling boring machine cutterhead with cracks. *Eng. Fail. Anal.* 141, 106669. doi:10.1016/j.engfailanal.2022.106669

Liu, Y., Sun, Z., and Zhou, R. (2015). On driving torque calculation of EPBM cutter head in complex strata. *Track Traffic and Undergr. Eng.* 33 (06), 83–85+90. doi:10.3969/j.issn.1009-7767.2015.06.027

Liu, J., Bin, H., and Guo, W. (2018). Load characteristics of the TBM cutterhead under mixed-face rock ground condition. *Harbin Gongcheng Daxue Xuebao/Journal Harbin Eng. Univ.* 39 (3), 575–583. doi:10.11990/jheu.201609049

Liu, B., Yang, H., and Karekal, S. (2020). Reliability analysis of TBM disc cutters under different conditions. *Undergr. Space* 6 (2), 142–152. doi:10.1016/j.undsp.2020.01.001

Nelson, P. P., Al-Jalil, Y. A., and Laughton, C. (1992). "Analysis of performance measures of tunnel boring machines," in *Rock characterization: ISRM symposium, eurock '92* (Chester, UK), 408–413.

Ramoni, M., and Anagnostou, G. (2010). Thrust force requirements for TBMs in squeezing ground. *Tunn. Undergr. Space Technol.* 25 (4), 433–455. doi:10.1016/j.tust.2010.02.008

Ruyong, D. (2018). *Study on the Mechanism and disposal Measures of clay Clogging in TBM cutter-head.* Master's thesis. Southwest jiaotong university.

Shen, X., Yuan, D., Jin, D., Chen, X., Luo, W., Peng, Y., et al. (2025). Model test on cutterhead-soil interaction during shield tunneling and its theoretical model. *Undergr. Space* 20, 46–68. doi:10.1016/j.undsp.2024.03.006

Shi, H., Yang, H., Gong, G., and Wang, L. (2011). Determination of the cutterhead torque for EPB shield tunneling machine. *Automation Constr.* 20 (8), 1087–1095. doi:10.1016/j.autcon.2011.04.010

Sun, W., Shi, M., Zhang, C., Zhao, J., and Song, X. (2018). Dynamic load prediction of tunnel boring machine (TBM) based on heterogeneous *in-situ* data. *Automation Constr.* 92, 23–34. doi:10.1016/j.autcon.2018.03.030

Wang, L., Gong, G., Shi, H., and Yang, H. (2012). Modeling and analysis of thrust force for EPB shield tunneling machine. *Automation Constr.* 27, 138–146. doi:10.1016/j.autcon.2012.02.004

Wang, X., Yuan, D., Jin, D., Jin, H., Yang, Y., and Wu, J. (2022). Determination of thrusts for different cylinder groups during shield tunneling. *Tunn. Undergr. Space Technol.* 127, 104579. doi:10.1016/j.tust.2022.104579

Yongjian, T. (2020). *Study on large-diameter slurry shield Tunneling with half-chamber Air pressure Method in Clay strata.* Master's thesis. Shanghai Jiaotong University.

Zhang, Q., Qu, C., Cai, Z., Kang, Y., and Huang, T. (2014). Modeling of the thrust and torque acting on shield machines during tunneling. *Automation Constr.* 40, 60–67. doi:10.1016/j.autcon.2013.12.008

Zhang, Q., Hou, Z., Huang, G., Cai, Z., and Kang, Y. (2015). Mechanical characterization of the load distribution on the cutterhead–ground interface of shield tunneling machines. *Tunn. Undergr. Space Technol.* 47, 106–113. doi:10.1016/j.tust.2014.12.009

Zhang, Q., Su, C., Qin, Q., Cai, Z., Hou, Z., and Kang, Y. (2016). Modeling and prediction for the thrust on EPB TBMs under different geological conditions by considering mechanical decoupling. *Sci. China Technol. Sci.* 59 (9), 1428–1434. doi:10.1007/s11431-016-6096-0

Zhang, J., Kou, L., Wang, J., and Xu, J. (2025). Load model for shield tunneling in composite strata considering mud build-up effects. *Tunn. Undergr. Space Technol.* 165, 106918. doi:10.1016/j.tust.2025.106918

Zhao, J., Gong, Q. M., and Eisensten, Z. (2007). Tunnelling through a frequently changing and mixed ground: a case history in Singapore. *Tunn. Undergr. Space Technol.* 22 (4), 388–400. doi:10.1016/j.tust.2006.10.002

Zhao, Y., Yang, H., Chen, Z., Chen, X., Huang, L., and Liu, S. (2019). Effects of jointed rock mass and mixed ground conditions on the cutting efficiency and cutter wear of tunnel boring machine. *Rock Mech. Rock Eng.* 52 (5), 1303–1313. doi:10.1007/s00603-018-1667-y

Zhou, X.-P., and Zhai, S.-F. (2018). Estimation of the cutterhead torque for earth pressure balance TBM under mixed-face conditions. *Tunn. Undergr. Space Technol.* 74, 217–229. doi:10.1016/j.tust.2018.01.025

Zhu, L., Zheng, Z., and Li, R. (2014). Calculation of shield cutter head torque in mix ground. *Mech. Eng. and Automation* (06), 110–111. doi:10.3969/j.issn.1672-6413.2014.06.044